Journal of Biomechanics ∎ (∎∎∎∎) ∎∎∎–∎∎∎

Contents lists available at ScienceDirect

Journal of Biomechanics

journal homepage: www.elsevier.com/locate/jbiomech
www.JBiomech.com

Wide bandwidth nanomechanical assessment of murine cartilage reveals protection of aggrecan knock-in mice from joint-overuse

Mojtaba Azadi [a,e,f,*,1], Hadi Tavakoli Nia [c,1], Stephanie J. Gauci [d], Christine Ortiz [b], Amanda J. Fosang [d], Alan J. Grodzinsky [e,f,g]

[a] School of Engineering, College of Science and Engineering, San Francisco State University, San Francisco, CA 94132, United States
[b] Department of Materials Science and Engineering, Massachusetts Institute of Technology, Cambridge, MA 02139, United States
[c] Massachusetts General Hospital, Harvard Medical School, Cambridge, MA 02139, United States
[d] University of Melbourne Department of Pediatrics & Murdoch Children's Research Institute, Parkville, Australia
[e] Center for Biomedical Engineering, Massachusetts Institute of Technology, Cambridge, MA 02139, United States
[f] Department of Biological Engineering, Massachusetts Institute of Technology, Cambridge, MA 02139, United States
[g] Department of Electrical Engineering and Computer Science, Massachusetts Institute of Technology, Cambridge, MA 02139, United States

ARTICLE INFO

Article history:
Accepted 28 March 2016

ABSTRACT

Aggrecan loss in human and animal cartilage precedes clinical symptoms of osteoarthritis, suggesting that aggrecan loss is an initiating step in cartilage pathology. Characterizing early stages of cartilage degeneration caused by aging and overuse is important in the search for therapeutics. In this study, atomic force microscopy (AFM)-based force–displacement micromechanics, AFM-based wide bandwidth nanomechanics (nanodynamic), and histologic assessments were used to study changes in distal femur cartilage of wildtype mice and mice in which the aggrecan interglobular domain was mutated to make the cartilage aggrecanase-resistant. Half the animals were subjected to voluntary running-wheel exercise of varying durations. Wildtype mice at three selected age groups were compared. While histological assessment was not sensitive enough to capture any statistically significant changes in these relatively young populations of mice, micromechanical assessment captured changes in the quasi-equilibrium structural-elastic behavior of the cartilage matrix. Additionally, nanodynamic assessment captured changes in the fluid–solid poroelastic behavior and the high frequency stiffness of the tissue, which proved to be the most sensitive assessment of changes in cartilage associated with aging and joint-overuse. In wildtype mice, aging caused softening of the cartilage tissue at the microscale and at the nanoscale. Softening with increased animal age was found at high loading rates (frequencies), suggesting an increase in hydraulic permeability, with implications for loss of function pertinent to running and impact-injury. Running caused substantial changes in fluid–solid interactions in aggrecanase-resistant mice, suggestive of tissue degradation. However, higher nanodynamic stiffness magnitude and lower hydraulic permeability was observed in running aggrecanase-resistant mice compared to running wildtype controls at the same age, thereby suggesting protection from joint-overuse.

1. Introduction

Osteoarthritis (OA), a musculoskeletal disease for which there are currently no disease modifying drugs, is a leading cause of disability worldwide, affects aging populations as well as young people with acute joint injuries (Hunter, 2011). In addition to age and traumatic joint injury, risk factors contributing to development and progression of include gender, obesity and metabolic factors, mechanical/anatomical factors, overuse, congenital deformities, and genetic predisposition (Goldring and Otero, 2011; Teeple et al., 2013; Goldring and Marcu, 2009). Cartilage degeneration in OA involves the initial loss of aggrecan and the degradation of the type II-IX-XI collagen network (Caterson et al., 2000) of the extracellular matrix (ECM). Loss of aggrecan and surface collagen fibrillation occur at the earliest stage of OA and evolve from molecular-level to tissue-scale changes. Detection of these early stages of degeneration is of great importance for understanding the molecular mechanisms of progression and potential therapeutic interventions to halt the progress of OA. However, conventional macroscale biomechanical assessment methods are often not sensitive enough to the earliest molecular changes in the ECM (Nia et al., 2013).

* Corresponding author.
E-mail address: Azadi@sfsu.edu (M. Azadi).
[1] contributed equally to this work.

http://dx.doi.org/10.1016/j.jbiomech.2016.03.055
0021-9290/

The use of appropriate animal models to aid in the assessment of OA-related risk factors and mechanisms, and to enable multiscale assessment of intrinsic material parameters is key to comprehensive understanding of OA pathophysiology. Among the available animal models of OA (Teeple et al., 2013; Little and Smith, 2008; Bendele, 2002), mouse models offer the unique potential to incorporate genetic manipulations that can control specific molecular mechanisms and cell signaling pathways associated with OA initiation and progression (Little and Hunter, 2013; Young, 2005; Fang and Beier, 2014). Murine models also offer a relatively inexpensive approach and they exhibit reproducible, detectable and relatively fast disease progression (Bendele, 2002; Little and Smith, 2008). Histological evaluation using various scoring systems is a critically important assessment tool to characterize cartilage changes (Aigner et al., 2010; Little and Zaki, 2012). Biomarkers, imaging techniques (e.g., micro-CT), pain assessment, and gait analysis can also provide useful outcome measures in the study of murine models of OA (Teeple et al., 2013; Fang and Beier, 2014).

In the present study, atomic force microscopy (AFM)-based force–displacement micromechanics, AFM-based nanodynamic high-bandwidth rheology, and histologic assessments were used to study changes in distal femur cartilage of wildtype mice and mice in which the aggrecan interglobular domain was mutated to make the cartilage aggrecanase-resistant. Half the animals were subjected to voluntary running-wheel exercise of varying durations. Wildtype mice at three selected age groups were compared. In general, macro-, micro- and nano-scale biomechanical tests are also used for quantitative assessment of time-independent and time-dependent properties of cartilage from animal models. For very thin ($\sim$50 μm) murine knee cartilage, micro-scale AFM-based force–displacement indentation can focus mainly on structural elasticity of the ECM (Batista et al., 2014; Stolz et al., 2009; Han et al., 2011). However, more recently developed AFM-based nanodynamic high bandwidth indentation tests can capture time-dependent poroelastic properties of murine cartilage as well, e.g., that from normal GAG-depleted murine cartilage (Nia et al., 2015a, 2015b), which shows high sensitivity in the detection of subtle changes associated with the earliest stages of OA. Here, histological, micromechanical and nanodynamic tests were implemented to detect the role of aggrecan, aging and substantial running on changes in murine knee cartilage using a well-established genetically engineered aggrecan knock-in mouse model compared to wildtype controls. The objective of this study was to quantitatively assess the consequences of genetic modification for aggrecanase resistance, aging and voluntary wheel running on the biomechanical properties of distal femur cartilage. We found that higher nanodynamic stiffness magnitude and lower hydraulic permeability was observed in the aggrecanase-resistant mice compared to wildtype controls at the same age, thereby showing protection from joint-overuse.

2. Materials and methods

2.1. Murine knee samples

24 knee joints dissected from eight 220 days old aggrecanase-resistant mice ("Jaffa") and 16 wildtype (WT) mice at 3 selected age groups of 100, 160 and 220 days (all C57BL/6 strain) were used in this study (i.e., six 100 day-old WT, five 160 day-old WT, five 220 day-old WT). As a result, the mice were relatively young, within one third of their normal life span. Jaffa has a mutation in the aggrecan interglobular domain that blocks ADAMTS cleavage at the [$E^{373}\downarrow^{374}A$] aggrecanase site (Little et al., 2007). Mice were allowed normal ambulation and those assigned to voluntary wheel running-mice were singly housed with constant access to one low-profile wireless running wheel (Med Associates). They could run ad-libitum from 6 weeks of age onwards when they were skeletally mature. Running mice consisted of three 100 day-old WT, three 160 day-old WT, two 220 day-old WT and five 220 day-old Jaffa. The distance traveled by each mouse was recorded automatically by software collected via a USB interface hub for wireless wheels (Med Associates). Different patterns of running were recorded; for example, some mice stopped running for several days then resumed. Distance traveled per day and total distance traveled varied for each animal. The range of the distance travelled for the 3 age groups of 100, 160 and 220 day-old mice were 283–734 km, 616–1503 km and 841–1851 km, respectively.

Mice not subjected to running wheels (non-running mice) were used as controls for statistical analysis in detecting the effect of joint-overuse, and wildtype mice were controls for genetically engineered mice at all three ages tested. Animal weight, age and the total distance run on the exercise wheel were recorded for each animal; these sample parameters were blind-coded for all assessments. Four histological assessments: cartilage erosion and aggrecan loss scoring on right knee tibia and femoral condyles were done as described in details in (Little et al., 2007). Hind left legs were disarticulated at the hip joint following euthanasia, preserved in −20 °C, and shipped in dry ice from Melbourne, AU to Cambridge, MA, USA. Joints were stored at −20 °C until dissection on the day of AFM experiments. Two AFM-based assessments, micromechanical force–displacement and nanodynamic complex modulus magnitude and phase, were performed on left knee medial femoral condyles. After data collection was completed, animal codes were unblinded for the purpose of grouping for statistical analysis.

2.2. Preparation of murine knee samples for AFM-based assessments

Before AFM experiments, the frozen left legs were thawed in a PBS bath containing protease inhibitors (Roche, Complete inhibitor cocktail). Freezing and thawing did not affect the biomechanical properties of the cartilage tissues studied in (Changoor et al., 2010; Szarko et al., 2010), as measured by traditional macroscopic tests. The knees were carefully dissected to remove nearby soft tissues (i.e. fat tissue, the quadriceps tendon and other collateral tendons from the end on the femur, the anterior cruciate ligament (ACL) and posterior cruciate ligament (PCL)) from the condyles which would otherwise block access of the AFM tip to the condyle surface. The remaining attachments of the ACL and PCL between the condyles were cut and the thin and transparent synovial membrane was removed by scraping the side surfaces of the joint. The cartilage surface was constantly moistened with protease inhibitor solution during sample preparation. AFM experiments were performed by 0.5–4 h after specimen preparation. To tailor the size of the sample to small space within the AFM, the head of the condyle was cut to a dimension of $\sim$3 mm using a handheld grinder, which enabled mounting the specimen on the substrate with the condyles facing upward. This approach placed the medial condyle slightly higher than the lateral condyle and facilitated indentation of the medial condyle.

2.3. AFM micromechanics and nanodynamics

Two AFM-based indentation experiments (micromechanics and nanodynamics were performed sequentially on the same AFM platform (Veeco Multimode AFM with Nanoscope IV and Picoforce MMAFMLN-AM controllers, Bruker Co.) equipped with a second extra high-bandwidth piezo actuator to measure the nano-scale complex modulus in the 1 Hz–10 kHz frequency range (Nia et al., 2015a; Nia et al., 2015c). An in-fluid probe holder (Bruker MTFML) was used for specimen mounting in the presence of protease inhibitor buffer (same buffer as above). This holder allowed visualization of the sample via an optical microscope. AFM tips were made by gluing (M-Bond 610, Micro measurements, Wendell, NC) spherical particles ($D = 22.6 \pm 0.7$ μm, Polybead®, Polysciences, Inc.) onto tipless cantilevers with nominal stiffness of 40 N/m (AIO-TL Innovative Solutions Bulgaria Ltd., Sofia, Bulgaria) using a separate AFM (MFP-3D-BIO AFM, Asylum Research, Santa Barbara, CA). The stiffness of all cantilevers was measured prior to particle attachment using the thermal noise method, and ranged between 26 and 53 N/m.

2.3.1. AFM-based micromechanics

Conventional AFM-based micro-scale indentation experiments were performed by displacing the cartilage sample toward the AFM tip at very slow speed ($\leq$ 1 μm/s) via the AFM z-piezo until a tip deflection of $\sim$50 nm was achieved (equivalent to a surface contact force of $\sim$2 μN), causing a tip displacement into the cartilage of $\sim$2–4 μm. Both loading and unloading force–displacement curves (FDC, e.g., Fig. 1b) were captured at $>$5 locations along the cartilage surface. The micro-scale quasi-equilibrium elastic modulus (E_{micro}) was calculated by fitting the Hertzian contact mechanics model to the indentation approach data.

2.3.2. AFM-based nanodynamic complex moduli

The nanodynamics protocol for measuring the magnitude and phase of the complex modulus of cartilage over a frequency range of 0.2 Hz–10 kHz has been described for bovine cartilage (Nia et al., 2013) and murine knee cartilage (Nia et al., 2015a) as well as aggrecan molecules (Nia et al., 2015c) extracted from bovine and human knee cartilage. Nanodynamics experiments were performed immediately after micro-scale force–displacement tests on the same joint surface locations without moving the tip position. A ramp-and-hold displacement into the cartilage of $\sim$2–4 μm is first applied, yielding a preload of $\sim$2 μN (Fig. 1c). After a pause for

Please cite this article as: Azadi, M., et al., Wide bandwidth nanomechanical assessment of murine cartilage reveals protection of aggrecan knock-in mice from joint-overuse. Journal of Biomechanics (2016), http://dx.doi.org/10.1016/j.jbiomech.2016.03.055

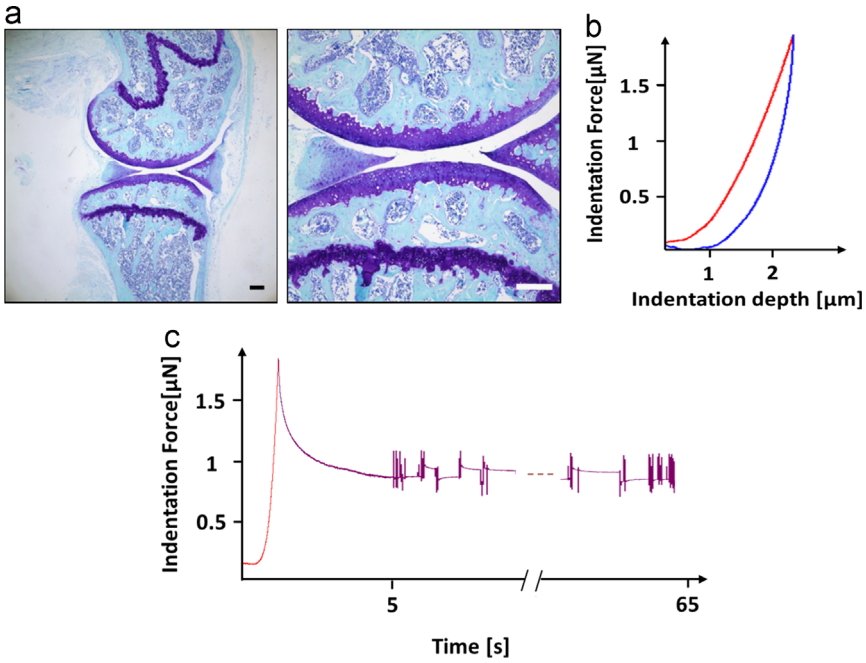

Fig. 1. Three assessments of 24 knee joints dissected from eight 220 days old aggrecanase-resistant mice ("Jaffa") and 16 wildtype (WT) (i.e., six 100 day-old WT, five 160 day-old WT, five 220 day-old WT) include histological scoring of right knee joints, AFM-based micromechanical (force–displacement indentation) assessment and AFM-based nanodynamic (wide bandwidth dynamic complex modulus) of left knee distal femur cartilage (a) Representative histological image of a Jaffa control (non-running) mouse cartilage (scale bar=200 μm) stained with toluidine blue. Cartilage erosion scoring and aggrecan loss scoring of right knee femoral and tibial condyles were performed; (b) An example of an AFM-based force versus depth micro indentation curve used to find the microscale quasi-equilibrium elastic modulus (E_{micro}) calculated by fitting a Hertzian contact model to the approach curve; (c) An example of nanodynamic indentation force curve measured directly after the micro-scale force–displacement test and subsequent stress relaxation by applying a random binary sequence pulse waveform for 60 s covering the frequency range of 0.1 Hz–10 kHz. The 60 s indentation force response is used, along with the applied displacement, to calculate the magnitude and phase of the complex indentation modulus versus frequency, as shown in Fig. 2. (For interpretation of the references to color in this figure legend, the reader is referred to the web version of this article.)

Table 1
List of the quantitative parameters used in this manuscript. Micromechanical parameter is found from micro-scale indentation curve (e.g. Fig. 1b) and nanodynamical parameters extracted from wide-bandwidth curves (e.g. Fig. 2) found by analyzing nanodynamical indentation curve (e.g. Fig. 1c).

Parameter		Description	Units
Micromechanical parameter (Micro-scale)	E_{micro}	Quasi-equilibrium elastic modulus	Pa
Nanodynamical parameters (Nano-scale)	E_{nano_L}	Low frequency elastic modulus	Pa
	E_{nano_H}	High frequency elastic modulus	Pa
	E_{nano_H}/E_{nano_L}	Self stiffening	–
	f_p	Peak frequency	Hz
	ϕ_p	Peak angle	Deg
	E_{nano_f}	Elastic modulus of the fibril network	Pa
	k	Hydraulic permeability	$m^4/N.s$

stress relaxation (typically 5–10 s), the sample is displaced by a second piezo actuator using a random binary pulse sequence that moves that sample into the cartilage for duration of ~60 s. This applied input displacement by the second piezo (~20 nm amplitude) results in a contact force of 80–200 nN on sample found by the AFM tip deflection (e.g., Fig. 1c) leading to and actual cartilage indentation deformation of ~2–5 nm. Signals are analyzed using discrete Fourier transform analysis along with a Hertzian contact model for the spherical shape to calculate the magnitude and phase of the complex modulus of the cartilage). In the experiments on murine cartilage reported here, instrumentation noise and drift was observed above ~2 kHz; we therefore focused on responses below 2 kHz in the results below.

2.3.3. Finite element modeling

Material parameters (See Table 1) directly calculated from the data are the low frequency elastic modulus (E_{nano_L}), the high frequency modulus (E_{nano_H}), the peak frequency (f_p) of the phase angle and the value of the phase at this peak (ϕ_p). A fibril-reinforced poroelastic model (Soulhat et al., 1999) has been implemented in which cartilage is approximated as a composite composed of an isotropic non-fibrillar matrix (representing the proteoglycan constituents), a fibril network (representing collagen fibrils) and a fluid phase (representing the water/electrolyte solution). This model has been implemented by using the axisymmetric poroelastic element (CAX4P) of the commercial finite element software ABAQUS (Version 6.14, SIMULIA, Providence, RI). The AFM probe tip, made out of polystyrene, was treated as a rigid solid since polystyrene (E~3 GPa) is much stiffer than cartilage (E~0.1–0.5 MPa). We assumed the indenter and the subchondral bone surface to be impermeable to fluid flow, and the indenter-cartilage contact region to be frictionless (Nia et al., 2011).We set the pore pressure to zero at the top surface of the cartilage (excluding the indenter contact surface) to simulate free draining of the interstitial fluid from the cartilage.

The relevant mechanical properties to be estimated are the Young's modulus E_{nano_L}, Poisson's ratio ν and the hydraulic permeability k of the nonfibrillar matrix and the Young's modulus of the fibril network, E_{nano_f} As a first approximation, it is assumed that the fibers resist only tension, and the compressive modulus for the fibers is set to zero (Soulhat et al., 1999) To determine these parameters, first, the low-frequency asymptote of the model was set equal to that of the experimental data, E_{nano_L} (in a parametric study in our previous work, we showed that varying the parameters E_{nano_f}, k and the Poisson's ratio ν did not affect the low-frequency asymptote E_{nano_L} (Nia et al., 2011) Then, E_{nano_L} fixed, the high-frequency asymptote was found to depend only on E_{nana_f} (see the parametric study section in (Nia et al., 2011). Therefore, E_{nano_f} was obtained by fitting the high-frequency asymptote of the model to that of the experimental data. Finally, the hydraulic permeability k was obtained by matching the frequency of the peak of the theoretical phase angle to that of the data, since varying the permeability only shifted the frequency dependence of $|E^*|$ and ϕ, and kept all the other parameters unchanged (see the parametric study section in (Nia et al., 2011). In this study, we used the Poisson's ratio of ν=0.1, the value measured previously for young bovine femoropatellar groove cartilage (Eisenberg and Grodzinsky, 1985).

2.3.4. Statistics

The measured micromechanical and nanodynamic parameters were quite repeatable at the same indentation location, resulting in output parameters with less than 5% difference for repeated experiments. To account for variations with location along the joint surface, n~5 locations were tested on each joint. Frequency-dependent self-stiffening (i.e., increasing modulus magnitude from low to high frequency) was observed in all samples as exemplified by the data of Fig. 2a.

Please cite this article as: Azadi, M., et al., Wide bandwidth nanomechanical assessment of murine cartilage reveals protection of aggrecan knock-in mice from joint-overuse. Journal of Biomechanics (2016), http://dx.doi.org/10.1016/j.jbiomech.2016.03.055

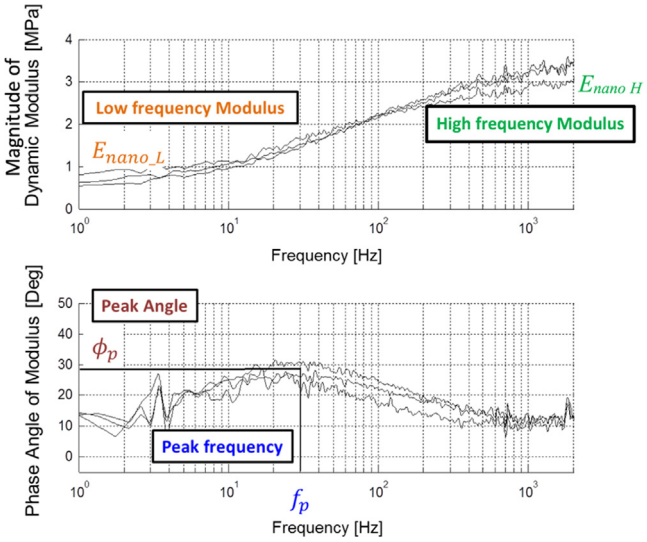

Fig. 2. Representative analyzed data for a set of 3 nanodynamic output curves corresponding to measurements done at 3 different locations on a single distal femur surface using the random binary sequence methodology shown/described in Fig. 1c along with the Hertz contact model. (a) Magnitude of dynamic complex modulus versus frequency, showing the low (~1 Hz) and the high frequency (~2,000 Hz moduli, E_{nano_L} and E_{nano_H} respectively, identified at the low and high frequency plateaus of the data (i.e., plateaus that are consistent with the poroelastic model of the tissue; (b) Phase angle of dynamic complex modulus versus frequency, showing the peak angle ϕ_P (~30° in this Data) and peak frequency f_P (~30 Hz in the presented data) values that are extracted from these data.

In addition, a clear peak in the phase angle could be observed (e.g., Fig. 2b). A generalized linear mixed effects model was used for statistical analysis of micromechanical and nanodynamic data with animal treated as a random effect and age and/or genotype considered as fixed effects. For assessment of histological differences, the Wilcoxon–Mann–Whitney test was used. A significance level of 5% ($p < 0.05$) was used for all analyses.

3. Results and discussion

In the following key findings and results are discussed. Additional data and results of statistical analyses are included in Supplementary materials.

3.1. Micro and nano-scale stiffness parameters of wildtype mice decrease with age

For study of the effect of age on cartilage stiffness, 16 wildtype mice in 3 age groups were used: mice were 100 days (6 mice), 160 days (5 mice) and 220 days old (5 mice) at the time of sacrifice. Since these mice become skeletally mature at 6 weeks and can live for ~700 days (2 years), our study population was relatively young (in the first third of life span). Half of the mice were subjected to voluntary wheel running; however, running did not result in any statistically significant ($p < 0.05$) or weakly significant ($0.05 < p < 0.1$) trends in any micromechanical or nanodynamic parameters within each age groups of wildtype mice (See Table 1–3, Supplementary materials). Therefore, statistical analysis of effects of age combined running and non-running mice (See Table 4, Supplementary materials). E_{micro} measured by micromechanical force–displacement tests (Fig. 3) showed significant softening between 160 and 220 day-old mice ($p=0.007$). Three nano-scale indicators (i.e., the high frequency modulus magnitude E_{nanno_H}, peak angle ϕ_p, and self-stiffening ratio defined as (E_{nano_H}/E_{nano_L}), showed consistent decreases from the youngest to oldest age groups Fig. 4a–c. The change in peak angle (Fig. 4b) indicates the loss of energy dissipation between the oldest and youngest wildtype mice, and the self-stiffening ratio (Fig. 4c)

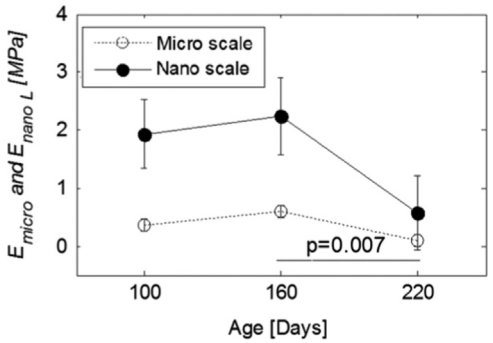

Fig. 3. Micromechanical modulus E_{micro} shows tissue softening with increasing age between the 160 day ($n=5$) and 220 day-old mice ($n=5$) ($p=0.007$). While low frequency modulus (E_{nano_L}) shows the same trend, differences with age were not statistically significant. The values of E_{micro} and E_{nano_L} are of the same order of magnitude and show the same patterns, though E_{nano_L} is always higher than E_{micro}, likely due to the depth-dependent heterogeneity of the tissue and differences in the measurement techniques.

shows a softening effect from youngest to both middle age ($p=0.052$) and oldest aged wildtype mice ($p=0.032$). These changes imply a decrease in the ability of fluid–solid frictional interactions to increase intra-tissue hydrostatic pressurization with increasing age, an effect that is needed to protect cartilage during high loading rate activities and to resist impact-injury. Age was found to be a very strong effect, as changes in mechanical parameters were detectable even when studied on all the samples by pooling same-age running, non-running, wildtype and Jaffa mice: significant decreases between the youngest and oldest mice were found after this grouping for all micro-scale and nano-scale parameters (i.e., E_{micro} $p=0.02$, E_{nano_H} $p=0.006$, E_{nano_H}/E_{nano_L} $p=0.001$, ϕ_p $p=0.02$, f_p $p=0.05$).

3.2. Quasi-equilibrium structural properties of cartilage were similar at the micro- and nano-scale

Data collected in the age study above also enabled comparison of quasi-equilibrium cartilage stiffness values measured first by micro-scale, low-rate force–displacement tests (E_{micro}) and then by nano-scale low frequency indentation (E_{nano_L}). The results of Fig. 3 suggest that, while E_{nano_L} was somewhat more than E_{micro}, they were both within the same order of magnitude. Such modest differences may be expected, since E_{micro} is measured from quasi-static force–displacement tissue indentations of d_o~2–4 μm, while E_{nano_L} is derived from dynamic indentation peak-to-peak amplitudes of only ~2 nm, performed at an initial offset displacement of d_o~2–4 μm at the low frequency limit of 1 Hz (Fig. 1c). Since the conventional micromechanical elasticity (E_{micro}) is found by fitting a Hertzian mechanics model that assumes cartilage is a homogeneous material with a single elastic modulus throughout the indentation depth d_o, E_{micro} represents an average value over depth d_o. In contrast, E_{nano_L} represents the magnitude of the quasi-static cartilage modulus at the exact position, d_o. Thus, these differences may be associated with the known depth dependent changes in cartilage moduli (e.g., as shown previously for bovine and porcine cartilage (Schinagl et al., 1997; McLeod et al., 2013), anisotropy due to distribution and orientation of collagen fibers (Ateshian et al., 2009; Taffetani et al., 2015), and the possible effects of strain stiffening which, together, may contribute to apparent increases in murine cartilage stiffness as indentation depth d_o is increased, which we have recently observed in a separate pilot study of this phenomenon (Azadi et al., 2014).

Please cite this article as: Azadi, M., et al., Wide bandwidth nanomechanical assessment of murine cartilage reveals protection of aggrecan knock-in mice from joint-overuse. Journal of Biomechanics (2016), http://dx.doi.org/10.1016/j.jbiomech.2016.03.055

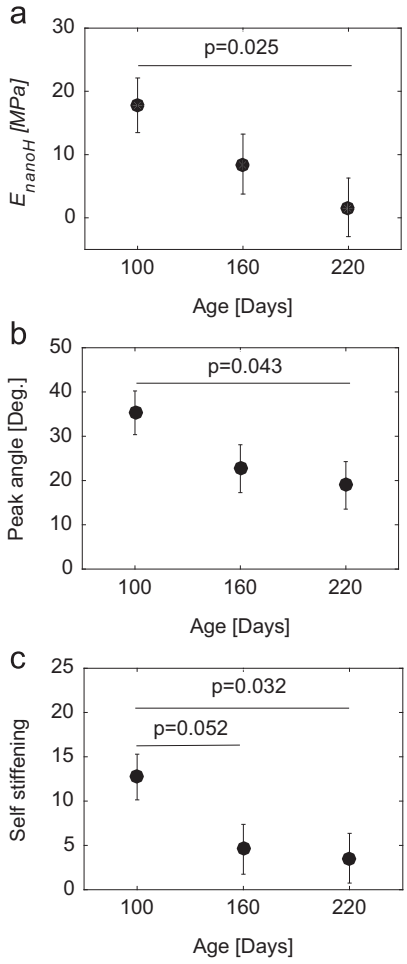

Fig. 4. Three nanodynamic indicators show the differences in wildtype cartilage material properties associated with age: (a) E_{nano_H}, the high frequency nano-mechanical modulus, (b) ϕ, the peak angle and (c) [E_{nano_H}/E_{nano_L}] the self-stiffening ratio. All three indicators decrease with increasing age. $n=6$, 5 and 5 for these 100, 160 and 220 day-old wildtype mice, respectively.

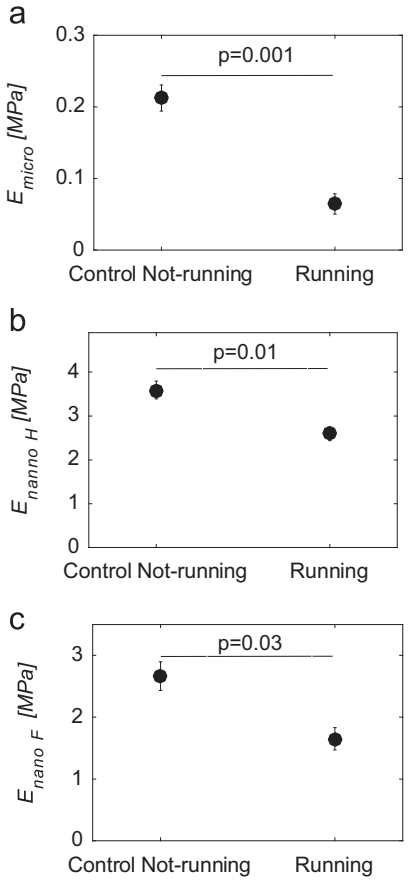

Fig. 5. Differences in micromechanical and nanodynamic cartilage material properties of voluntary wheel running ($n=5$) versus non-running ($n=3$) Jaffa mice. (a) Substantial running appears to cause softening of the cartilage of aggrecanase-resistant mice at the micro-scale (E_{micro}); Substantial running also caused substantial changes in fluid–solid interactions manifest in the decrease of the high frequency nanodynamic stiffness (b) E_{nano_H}, and a decrease in the fiber modulus calculated from the fibril reinforced poroelastic modulus (c) E_{nano_F}.

3.3. Non-wheel running genetically engineered and wildtype murine cartilage had similar stiffness

Micromechanical and nanodynamic properties as well as histological scores of distal femur cartilage of non-running genetically engineered mice (Jaffa) were compared to the properties of the corresponding non-running wildtype controls. The nanodynamic hydraulic permeability and the elastic modulus of the fibril network (E_{nano_f}) were calculated for same-aged Jaffa and wildtype mice (220 day-old) using fibril-reinforced poroelastic model, described above. Only the same-age, non-running mice were used, initially, to identify any effects of gene modification (to eliminate any confounding effects of age and running). No statistical differences were found between the mechanical properties or histological scores of non-running Jaffa mice with their corresponding same-aged non-running wildtype controls. This result indicates that the mechanical properties of these aggrecanase resistant mice, when not loaded excessively by long distance running, are similar to those of wildtype mice.

3.4. Effect of long distance running and potential joint overuse

3.4.1. Long distance running affected the aggrecanase protected but not wildtype knee cartilage

The effects of voluntary wheel running and genetic mutation on both the micromechanical and nanodynamic mechanical properties of 220 day murine distal femur cartilage were compared. For this group of wildtype controls (220 day-old), no significant differences were associated with wheel running. However, running had a very clear effect on both micro- and nanoscale mechanical properties of Jaffa mice which, at 220 days-old had run the longest distances (841– 1 851 km) (Fig. 5, see Table 5, Supplementary materials for detailed data). The lower E_{micro} of Jaffa wheel running mice (Fig. 5a) suggests structural softening of Jaffa knee cartilage associated with long distance running. Furthermore, the decrease in high frequency nano-scale modulus (E_{nano_H}, Fig. 5b) and the elastic modulus of the fibrillar network (E_{nano_f}, Fig. 5c) indicate differences in fluid-interactions within the cartilage associated with long distance running and overuse in Jaffa mice leading to tissue softening and decreased ability to dissipate energy.

3.4.2. Aggrecanase protected mice were resistant to decreased stiffness at higher loading rates

When the mechanical properties of knee cartilage in wheel running Jaffa mice were compared with their corresponding wheel running wildtype controls (See Table 6, Supplementary materials), no differences were detected in micro-scale tests. However, nanodynamic tests revealed a difference in properties pertaining to fluid–solid interactions at high loading rates (frequencies): aggrecanase resistant cartilage showed a higher E_{nano_H} (Fig. 6a) and a lower hydraulic permeability, k, (Fig. 6b) compared to knee cartilage in wildtype controls. Thus, the aggrecanase protected

Please cite this article as: Azadi, M., et al., Wide bandwidth nanomechanical assessment of murine cartilage reveals protection of aggrecan knock-in mice from joint-overuse. Journal of Biomechanics (2016), http://dx.doi.org/10.1016/j.jbiomech.2016.03.055

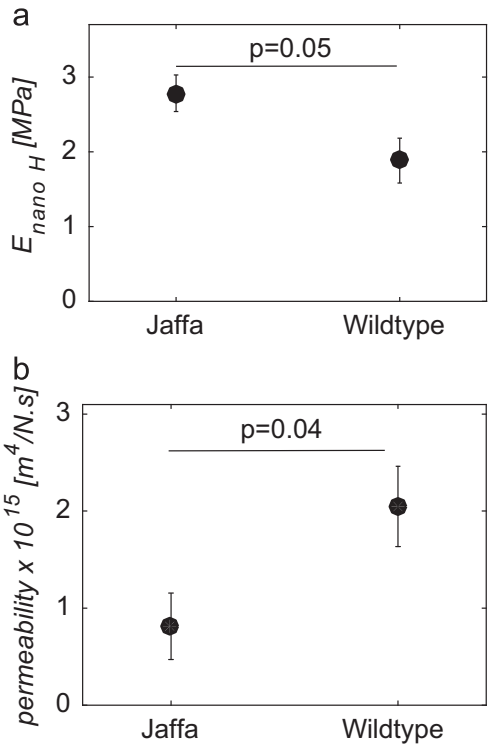

Fig. 6. Knee cartilage of Jaffa wheel running mice ($n=5$) showed higher stiffness than the cartilage of the corresponding running wildtype controls ($n=3$) at higher loading rates, as manifested in greater high frequency stiffness E_{nano_H} (a) and lower hydraulic permeability (b). Thus, Jaffa knee cartilage showed better protection against high loading rate activities.

cartilage in Jaffa mice presented better protection to high loading rate activities relevant to running and impact injury, as well as the ability to dissipate more energy at these high frequencies. Interestingly, these changes in ECM associated with substantial running (i.e., joint-overuse) were only detectable by high frequency nanodynamic tests capable of assessing E_{nano_H} and k, not by low frequency nanodynamic modulus E_{nano_L} or by micromechanical force–displacement tests (which can only assess the quasistatic structural parameter, E_{micro}. This finding is consistent with our previous report that focused on the contribution of aggrecan to the wide bandwidth rheology of murine distal femur cartilage (Nia et al., 2015a): in that study, loss of aggrecan GAG chains had a far more significant effect on E_{nano_H}, k, and cartilage self-stiffening than on the low frequency quasistatic modulus. If micro-scale structural changes in E_{micro} did occur, they were apparently too small to be detected.

4. Summary and conclusions

Subtle changes in relatively young murine distal femur cartilage associated with age and extensive wheel running did not result in detectable changes in histological appearance and, thus, no significant changes in histological scoring were detected using four histological scoring assessments on the femur and tibia. Nevertheless, AFM-based micromechanical and especially nanodynamic indentation tests were able to sensitively detect certain effects of both age and running in the comparison of aggrecanase protected (Jaffa) versus wildtype control mice. These AFM-based techniques enabled the quantitation of both structural properties (i.e., the time independent, quasi-equilibrium moduli, E_{micro} and E_{nano_L}) as well as poroelastic (time-dependent) properties associated with fluid–solid interactions and pressurization within cartilage (embodied in the parameters, E_{nano_H}, k, and the self-stiffening ratio, $[E_{nano\_H}/E_{nano\_L}]$). These higher frequency poroelastic properties could only be assessed via wide bandwidth AFM nanoindentation tests in spite of the small size of the mouse knee joint and the thin layer of cartilage ($<$ 50 μm).

While conventional force–displacement (low frequency) microindentation methods could capture matrix structural information in knee cartilage, these tests could not measure fluid–solid interactions that are dominant at higher loading rates corresponding to running, jumping and traumatic joint injury (Nia et al., 2011, 2015a). These high loading rate activities of cartilage specifically involve the ability of cartilage matrix aggrecan molecules and aggrecan GAG chains and the very small GAG–GAG separation distances (~3 nm spacing within the ECM) that is the basis of cartilage's high resistance to fluid flow and the associated low value of the hydraulic permeability in normal cartilage. Compression of cartilage causes intra-tissue fluid flow that becomes more and more prominent as the frequency of compression increases. The AFM-based nanodynamic assessment techniques described here could sensitively detect changes in these high loading rate properties and proved to be more sensitive than micromechanical force–displacement measurements.

Loss of pressurization and drop in peak angle with aging, imply softening of the cartilage tissue and a possible increase of permeability due to aging at higher frequencies pertinent to walking, running and impact-injury. Loss of aggrecan will generally cause cartilage to be softer, particularly during high frequency loading. Results showed that the aggrecanase protected cartilage (Jaffa) presented better protection to high loading rate activities relevant to running and impact injury. Therefore, we believe that the results comparing aggrecanase protected (Jaffa) mice with wildtype mice suggests the possibility that this system can reveal early changes in cartilage mechanical properties associated with long-term joint use (age and exercise) and the effects of extracellular matrix composition change due to gene modification or molecule deletion on joint function. Substantial running might cause substantial changes in fluid–solid interactions and the possibility of aggrecan loss, even in aggrecanase-resistant mice. Thus, age as well as the intensity of running should appear to have a profound influence on the ECM.

The proposed methodologies developed in this study can be used for other studies that involve genetically engineered mice as well as other small animal models. In addition, the novel AFM based nanodynamic methodology can be used for other time-dependent biomaterials that exhibit viscoelastic or poroelastic behaviors including hydrogels, engineered tissues, ligament, meniscus and skin. These methods can be further used to compare the effect of drugs for blocking aggrecanases in cartilage and other soft tissues.

Conflict of interest statement

The authors have no conflicts to disclose.

Acknowledgments

The authors are grateful for the support of the Arthritis Australia and the U.S. National Institute of Health (NIH Grant AR060331) and National Science Foundation funding (DEB-0908187). Use of equipment in the Institute for Soldier Nanotechnologies and Center for Materials Science and Engineering at MIT is gratefully acknowledged.

Please cite this article as: Azadi, M., et al., Wide bandwidth nanomechanical assessment of murine cartilage reveals protection of aggrecan knock-in mice from joint-overuse. Journal of Biomechanics (2016), http://dx.doi.org/10.1016/j.jbiomech.2016.03.055

Appendix A. Supplementary material

Supplementary data associated with this article can be found in the online version at http://dx.doi.org/10.1016/j.jbiomech.2016.03.055.

References

Aigner, T., Cook, J.L., Gerwin, N., Glasson, S.S., Laverty, S., Little, C.B., McIlwraith, W., Kraus, V.B., 2010. Histopathology atlas of animal model systems – overview of guiding principles. Osteoarthr. Cartil. 18 (Suppl. 3), S2–S6.

Ateshian, G.A., Rajan, V., Chahine, N.O., Canal, C.E., Hung, C.T., 2009. Modeling the matrix of articular cartilage using a continuous fiber angular distribution predicts many observed phenomena. J. Biomech. Eng. 131, 061003.

Azadi, M., Nia, H.T., Grodzinsky, A.J., and Ortiz, C., 2014. Nonlinear nanomechanics of murine articular cartilage. In: Proceedings of the 2014 World Congress of Biomechanics, Boston: Curran Associates, Inc.

Batista, M.A., Nia, H.T., Önnerfjord, P., Cox, K.A., Ortiz, C., Grodzinsky, A.J., Heinegård, D., Han, L., 2014. Nanomechanical phenotype of chondroadherin-null murine articular cartilage. Matrix Biol. J. Int. Soc. Matrix Biol. 38, 84–90.

Bendele, A.M., 2002. Animal models of osteoarthritis in an era of molecular biology. J. Musculoskelet. Neuronal Interact. 2, 501–503.

Caterson, B., Flannery, C.R., Hughes, C.E., Little, C.B., 2000. Mechanisms involved in cartilage proteoglycan catabolism. Matrix Biol. J. Int. Soc. Matrix Biol. 19, 333–344.

Changoor, A., Fereydoonzad, L., Yaroshinsky, A., Buschmann, M.D., 2010. Effects of refrigeration and freezing on the electromechanical and biomechanical properties of articular cartilage. J. Biomech. Eng. 132, 064502.

Eisenberg, S.R., Grodzinsky, A.J., 1985. Swelling of articular cartilage and other connective tissues: electromechanochemical forces. J. Orthop. Res. Publ. Orthop. Res. Soc. 3, 148–159.

Fang, H., Beier, F., 2014. Mouse models of osteoarthritis: modelling risk factors and assessing outcomes. Nat. Rev. Rheumatol. 10, 413–421.

Goldring, M.B., Marcu, K.B., 2009. Cartilage homeostasis in health and rheumatic diseases. Arthritis Res. Ther. 11, 224.

Goldring, M.B., Otero, M., 2011. Inflammation in osteoarthritis. Curr. Opin. Rheumatol. 23, 471–478.

Han, L., Grodzinsky, A.J., Ortiz, C., 2011. Nanomechanics of the cartilage extracellular matrix. Annual Rev. Mater. Res. 41, 133–168.

Hunter, D.J., 2011. Pharmacologic therapy for osteoarthritis–the era of disease modification. Nat. Rev. Rheumatol. 7, 13–22.

Little, C.B., Hunter, D.J., 2013. Post-traumatic osteoarthritis: from mouse models to clinical trials. Nat. Rev. Rheumatol. 9, 485–497.

Little, C.B., Zaki, S., 2012. What constitutes an "animal model of osteoarthritis"–the need for consensus? Osteoarthr Cartil. OARS Osteoarthr. Res. Soc. 20, 261–267.

Little, C., Smith, M., 2008. Animal models of osteoarthritis. Curr. Rheumatol. Rev. 4, 175–182.

Little, C.B., Meeker, C.T., Golub, S.B., Lawlor, K.E., Farmer, P.J., Smith, S.M., Fosang, A.J., 2007. Blocking aggrecanase cleavage in the aggrecan interglobular domain abrogates cartilage erosion and promotes cartilage repair. J. Clin. Investig. 117, 1627–1636.

McLeod, M.A., Wilusz, R.E., Guilak, F., 2013. Depth-dependent anisotropy of the micromechanical properties of the extracellular and pericellular matrices of articular cartilage evaluated via atomic force microscopy. J. Biomech. 46, 586–592.

Nia, H.T., Han, L., Li, Y., Ortiz, C., Grodzinsky, A., 2011. Poroelasticity of cartilage at the nanoscale. Biophys. J. 101, 2304–2313.

Nia, H.T., Bozchalooi, I.S., Li, Y., Han, L., Hung, H.-H., Frank, E., Youcef-Toumi, K., Ortiz, C., Grodzinsky, A., 2013. High-bandwidth AFM-based rheology reveals that cartilage is most sensitive to high loading rates at early stages of impairment. Biophys. J. 104, 1529–1537.

Nia, H.T., Gauci, S., Azadi, M., Hung, H.-H., Frank, E., Fosang, A., Ortiz, C., Grodzinsky, A., 2015a. High-bandwidth AFM-based rheology is a sensitive indicator of early cartilage aggrecan degradation relevant to mouse models of osteoarthritis. J. Biomech. 48, 162–165.

Nia, H.T., Gauci, S.J., Hung, H.-H., Azadi, M., Frank, E., Fosang, A.J., Ortiz, C., and Grodzinsky, A.J., 2015b. High-bandwidth AFM-based rheology is a sensitive differentiator of GAG-depletion in mouse cartilage. In: Proceedings of 2014 Annual Meeting – Orthopaedic Research Society, pp. 162–165.

Nia, H.T., Han, L., Bozchalooi, I.S., Roughley, P., Youcef-Toumi, K., Grodzinsky, A., Ortiz, C., 2015c. Aggrecan nanoscale solid–fluid interactions are a primary determinant of cartilage dynamic mechanical properties. ACS Nano 9, 2614–2625.

Schinagl, R.M., Gurskis, D., Chen, A.C., Sah, R.L., 1997. Depth-dependent confined compression modulus of full-thickness bovine articular cartilage. J. Orthop. Res. 15, 499–506.

Soulhat, J., Buschmann, M.D., Shirazi-Adl, A., 1999. A fibril-network-reinforced biphasic model of cartilage in unconfined compression. J. Biomech. Eng. 121, 340–347.

Stolz, M., Gottardi, R., Raiteri, R., Miot, S., Martin, I., Imer, R., Staufer, U., Raducanu, A., Düggelin, M., Baschong, W., et al., 2009. Early detection of aging cartilage and osteoarthritis in mice and patient samples using atomic force microscopy. Nat. Nanotechnol. 4, 186–192.

Szarko, M., Muldrew, K., Bertram, J.E., 2010. Freeze–thaw treatment effects on the dynamic mechanical properties of articular cartilage. BMC Musculoskelet. Disord. 11, 231.

Taffetani, M., Raiteri, R., Gottardi, R., Gastaldi, D., Vena, P., 2015. A quantitative interpretation of the response of articular cartilage to atomic force microscopy-based dynamic nanoindentation tests. J. Biomech. Eng. 137 071005–071005.

Teeple, E., Jay, G.D., Elsaid, K.A., Fleming, B.C., 2013. Animal models of osteoarthritis: challenges of model selection and analysis. AAPS J. 15, 438–446.

Young, M.F., 2005. Mouse models of osteoarthritis provide new research tools. Trends Pharmacol. Sci. 26, 333–335.

Please cite this article as: Azadi, M., et al., Wide bandwidth nanomechanical assessment of murine cartilage reveals protection of aggrecan knock-in mice from joint-overuse. Journal of Biomechanics (2016), http://dx.doi.org/10.1016/j.jbiomech.2016.03.055